

This article was downloaded by: [University of Birmingham]

On: 10 February 2012, At: 05:19

Publisher: Taylor & Francis

Informa Ltd Registered in England and Wales Registered Number: 1072954 Registered office: Mortimer House, 37-41 Mortimer Street, London W1T 3JH, UK



Aerosol Science and Technology

Publication details, including instructions for authors and subscription information:

<http://www.tandfonline.com/loi/uast20>

Real-Time Measurements of Nonmetallic Fine Particulate Matter Adjacent to a Major Integrated Steelworks

Manuel Dall'Osto ^{a b}, Frank Drewnick ^c, Ray Fisher ^d & Roy M. Harrison ^{a e}

^a Division of Environmental Health and Risk Management, University of Birmingham, Birmingham, UK

^b Institute for Environmental Assessment and Water Research (IDÆA-CSIC), Barcelona, Spain

^c Particle Chemistry Department, Max-Planck-Institute for Chemistry, Mainz, Germany

^d Tata Steel Research, Development and Technology, Swinden Technology Centre Moorgate, Rotherham, UK

^e Centre of Excellence in Environmental Studies, King Abdulaziz University, Jeddah, Saudi Arabia

Available online: 06 Jan 2012

To cite this article: Manuel Dall'Osto, Frank Drewnick, Ray Fisher & Roy M. Harrison (2012): Real-Time Measurements of Nonmetallic Fine Particulate Matter Adjacent to a Major Integrated Steelworks, *Aerosol Science and Technology*, 46:6, 639-653

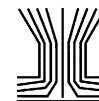
To link to this article: <http://dx.doi.org/10.1080/02786826.2011.647120>

PLEASE SCROLL DOWN FOR ARTICLE

Full terms and conditions of use: <http://www.tandfonline.com/page/terms-and-conditions>

This article may be used for research, teaching, and private study purposes. Any substantial or systematic reproduction, redistribution, reselling, loan, sub-licensing, systematic supply, or distribution in any form to anyone is expressly forbidden.

The publisher does not give any warranty express or implied or make any representation that the contents will be complete or accurate or up to date. The accuracy of any instructions, formulae, and drug doses should be independently verified with primary sources. The publisher shall not be liable for any loss, actions, claims, proceedings, demand, or costs or damages whatsoever or howsoever caused arising directly or indirectly in connection with or arising out of the use of this material.



Real-Time Measurements of Nonmetallic Fine Particulate Matter Adjacent to a Major Integrated Steelworks

Manuel Dall'Osto,^{1,2} Frank Drewnick,³ Ray Fisher,⁴ and Roy M. Harrison^{1,5}

¹Division of Environmental Health and Risk Management, University of Birmingham, Birmingham, UK

²Institute for Environmental Assessment and Water Research (IDÆA-CSIC), Barcelona, Spain

³Particle Chemistry Department, Max-Planck-Institute for Chemistry, Mainz, Germany

⁴Tata Steel Research, Development and Technology, Swinden Technology Centre Moorgate, Rotherham, UK

⁵Centre of Excellence in Environmental Studies, King Abdulaziz University, Jeddah, Saudi Arabia

A campaign took place in Wales (UK) in the spring of 2006 to characterize emissions from a major steelworks through atmospheric measurements. At no time during the measurements was the 24-h air quality standard for PM₁₀ exceeded. However, real-time measurements of single particles by aerosol time-of-flight mass spectrometry (ATOFMS) allowed detection of particulate matter from the steelworks, which could be associated with specific emission areas within the works from measurements of wind direction. Three main wind sectors were identified with possible sources of emissions of fine nonmetallic particulate matter (PM < 1 μm). Characterization of the aerosol composition by a high resolution time-of-flight aerosol mass spectrometer (HR-ToF-AMS) of the nonrefractory material associated with the specific plumes is also reported, along with results from other real-time techniques. The ATOFMS detected for the first time a unique elemental sulfur-rich particle type, likely to originate from the blast furnaces. AMS results, supported also by laboratory studies, confirm this finding by reporting elevated mass ratios *m/z* 64/48 and *m/z* 64/80. Two other novel ATOFMS particulate types were found to be associated with steelworks emissions. One was characterized by nitrogen-containing organic species, aromatic compounds, and high-molecular-weight (MW) polycyclic aromatic hydrocarbons (PAHs) and was associated with the sources in the area of the hot and cold mills. The second was found to be rich in organic carbon internally mixed with elemental carbon, nitrate, sulfate, and

PAHs with lower MW. These particle types were likely related to the coke ovens and the basic oxygen steelmaking plant.

1. INTRODUCTION

The iron and steel industry produces materials widely used to manufacture products that are essential for modern life and makes a major contribution to the economy of the EU. Steel is produced via two main routes: the electric arc furnace (EAF) process and the integrated steelmaking process. The EAF process is less complex since it is based on the re-melting of steel scrap using electrical energy supplied by striking an arc between carbon electrodes and the steel scrap. The integrated route, on the other hand, involves a number of closely linked processes whereby iron is extracted from its ores in the blast furnace and the resulting molten iron is subsequently converted into liquid steel in the basic oxygen steelmaking (BOS) process. The integrated process route also includes iron ore sintering and cokemaking facilities, which are used to prepare agglomerated iron ores and coke, respectively, for use in the blast furnace. In both the EAF and integrated steelmaking processes, the liquid steel may be further refined using secondary steelmaking processes and/or subject to vacuum degassing prior to being cast and rolled into various finished or semi-finished products. In some instances, the steel product is coated at these or other works with other metals such as zinc, tin, or organic materials to improve corrosion resistance. A more detailed description of the processes can be found elsewhere (Anderson and Fisher 2002).

The production of steel by the integrated process necessarily involves energy-intensive steps, producing significant CO₂ emissions (Kim and Worrell 2002). Although there have been a number of studies focused on dioxins (Anderson and Fisher 2002; Thompson et al. 2003; L.C. Wang et al. 2003; T. S. Wang et al. 2003; Aries et al. 2006), polycyclic aromatic hydrocarbons (PAHs) (Khalili et al. 1995; Yang et al. 1998, 2002; Choi

Received 15 August 2011; accepted 7 November 2011.

The authors acknowledge financial support from the European Union for the ULTRAFINE project (RFCS-CR-04049) under the Research Fund for Coal and Steel programme. The University of Birmingham also acknowledge financial support from Tata Steel R, D & T and the UK National Centre for Atmospheric Science (NCAS). Wayne Smith and Thomas Böttger are acknowledged for logistical and technical support during the field measurements. Sören Zorn is thanked for support during the ToF-AMS laboratory measurements.

Address correspondence to R. M. Harrison, Division of Environmental Health & Risk Management, University of Birmingham, Birmingham B15 2TT, UK. E-mail: r.m.harrison@bham.ac.uk

et al. 2007; Jiun-Hong et al. 2007), and trace metals (Ledoux et al. 2006; Mazzei et al. 2006; Choel et al. 2007), there are uncertainties associated with overall particulate matter (PM) emission rates, composition, and size distributions. Moreover, the chemical composition of PM emitted from such processes is variable and complex, which makes the study of the possible toxicology of these particles all the harder. In this respect, a variety of components has been proposed to induce inflammation, leading to adverse health effects (Dockery et al. 1993; Pope et al. 1995; Harrison and Yin 2000; Pope et al. 2002). The impact of the steel industry on chemical composition of ambient PM has been the subject of a number of studies: for example, Hutchison et al. (2005) reported an increase in the metal content of particles collected downwind of a steelworks and showed that these were in turn associated with increased inflammation of a rat's lungs. In a similar study, Pope (1996) reported a reduction in PM₁₀ mass concentrations and a decrease in the iron, copper, and zinc content of such particles during the period of closure of a steel mill in the Utah Valley.

Owing to the lack of adequate measurement technology, most investigations into the chemical composition of atmospheric PM consist of long-term measurements using 24-h average samples. However, several industrial emission sources are noncontinuous batch processes and long time-averaged ambient samples can mask the effects of short-term events, making it very difficult to characterize sources (Ogulei et al. 2005). Moreover, besides their low time resolution, traditional off-line filter-based techniques may suffer from sampling artifacts and hence provide very limited information on the mixing state of the particles. Weitkamp et al. (2005) reported fine particle emission profiles for a large coke production facility and stated that the variable wind direction did not guarantee by itself that the sampling site was influenced by the coking plant: other variables such as wind speed and mixing layer height also had to be taken into account. Oravisjarvi et al. (2003) also stressed the point that steel industry activities vary differently with time and the emissions have different release heights.

In recent years, aerosol mass spectrometry has emerged as a powerful tool for the on-line chemical characterization of individual aerosol particles (Murphy 2007) or small aerosol ensembles (Canagaratna et al. 2007). Therefore, in order to circumvent the problems of traditional off-line filter-based techniques mentioned above, two real-time mass spectrometers were deployed in the field in order to study the nature of PM in ambient air in the vicinity of an integrated steelworks. In particular, two types of aerosol mass spectrometer have been commercially available: the TSI aerosol time-of-flight mass spectrometer (ATOFMS, TSI 3800) and the Aerodyne aerosol mass spectrometer (AMS, Aerodyne Research Inc). The ATOFMS provides single-particle information on the abundance of different types of aerosol particles as a function of particle size with high time resolution. ATOFMS can be used to differentiate between particle sources (e.g., natural and anthropogenic) and particle age (reacted versus fresh sea salt) (Guazzotti et al. 2001) as well as to de-

termine the chemical mixing state (e.g., organics internally or externally mixed with inorganic species) of individual particles in real time (Noble and Prather 1996). The AMS quantifies mass concentrations of the nonrefractory aerosol components as well as species-resolved size distributions (Jayne et al. 2000; Canagaratna et al. 2007).

During the period 2004–2007, both these aerosol mass spectrometry techniques were deployed in a coordinated European research programme, ULTRAFINE, that was led by CORUS UK Limited, which aimed to characterize fine and ultrafine particulate emissions from integrated steelworks' operations. Particular focus was directed to tracing the source(s) of specific time events when relatively high concentrations of fine particulate matter were detected.

This work follows the findings reported in an earlier paper (Dall'Osto et al. 2008), where a discussion on the metallic constituents of particulate matter determined during this study was presented. Specifically, ATOFMS measurements showed six particle classes rich in alkali and trace metals associated with emissions from steelmaking processes. Two of these were iron-rich, one showing internal mixing with nitrate, the other internally mixed with phosphate, which subsequent analysis identified as arising from the ironmaking sector, with the hot and cold mills as the dominant sources, respectively. A micro-orifice uniform deposit impactor (MOUDI), used to measure particle size distributions over periods of 19–42 h, showed two characteristic size distributions for iron, one bimodal with modes at 0.45 μm and 4 μm , the other unimodal centered at 6 μm . In the former case, the smaller mode exhibited a peak for lead at the same particle size, and in the case of the larger mode, phosphate and calcium also showed a peak at 4- μm diameter, consistent with the ATOFMS findings. An additional particle type with a unimodal size distribution centered at about 1.2 μm , with internally mixed Pb, Zn, and Cl but not Fe, was also found.

The objective of this paper is to report additional ATOFMS particle types not previously reported in the literature and associated with steelworks activity. While the previous study was focused on metals and co-located ATOFMS-MOUDI results were presented, in this work, submicron particles detected with co-located AMS-ATOFMS measurements are presented. The advantage of the TSI-ATOFMS is that being a single-particle technique, it provides unique information for different particle types, resulting in an excellent tool for source apportionment studies of particulate matter. This is compensated by quantitative concentrations afforded by the HR-ToF-AMS and other techniques that were applied in the investigation. In summary, while the study of Dall'Osto et al. (2008) presented a detailed study of the size distribution and the metal chemical characterization of airborne particles in the vicinity of a large integrated steelworks, this study focuses on particle types with low metal content. Finally, a table summarizing this study and the one of Dall'Osto et al. (2008) is presented as concluding remarks.

2. EXPERIMENTAL METHODS

2.1. Sampling Site and Steelworks Sources

Sampling took place in the coastal town of Port Talbot, adjacent to one of the largest integrated steelworks in the UK. The sampling site chosen forms part of a UK national monitoring station that is located between the steelworks, to the southwest of the site and a major motorway to the east/northeast of the site. The proximity of the site to residential receptors can be seen in Figure 1, along with the locations of the main steelworks processes. Emissions from integrated steel-

making facilities consist of a complex mixture of stationary sources and fugitive emissions associated with the main processes, and fugitive emissions from general site activities such as the unloading, transport, stocking, and blending of particulate raw materials on site. This is further complicated by the fact that some processes operate continuously, whereas others are batch processes, some of which may involve parallel processing, thus giving the appearance of quasi-continuous operation.

Several studies have reported information derived from the sampling site used for this study, showing that a number of

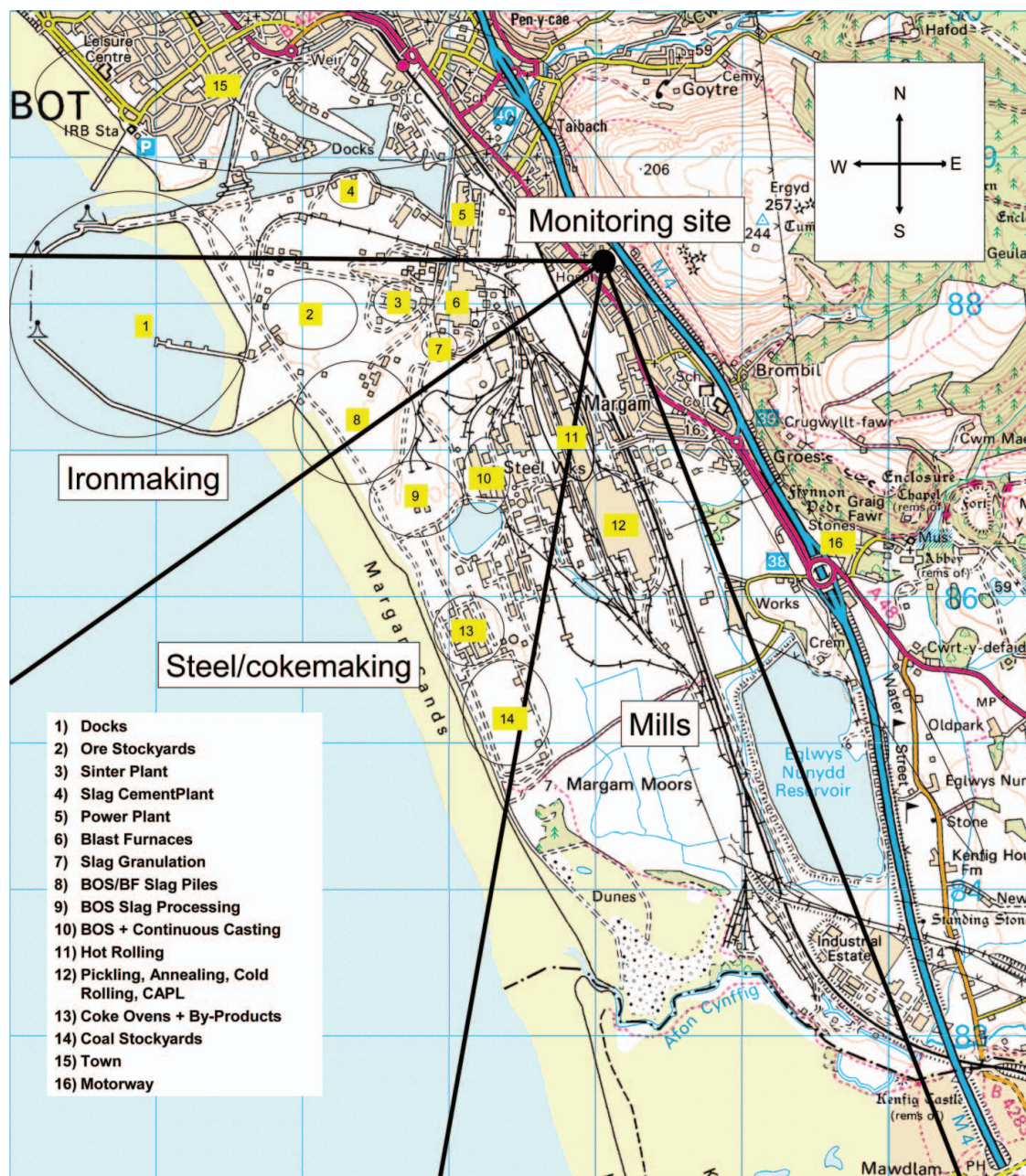


FIG. 1. Map of study area. (Color figure available online).

different atmospheric emission sources affect the site. Harrison and Jones (2005) reported a strong PM₁₀ source to the southwest and a strong NO_x source to the northeast. The PM₁₀ source was attributed to the steelworks, while the NO_x increment was ascribed to vehicular emissions on the motorway. Moreover, at the monitoring station, it was noticed that the sea breeze circulation favored the detection of PM₁₀ associated with the steelworks during the late afternoon. Moreno et al. (2004) deployed a high-volume cascade impactor collector in the same location: the sample cluster associated with the steelworks and the motorway showed the highest average collection rate (0.9 mg h⁻¹; 13 μg m⁻³). The smallest amount of total metals analyzed was found in samples associated with an urban origin in Port Talbot town.

The principal emission sources, the emissions' characteristics, and their components are summarized in Table 1.

2.2. Measurement Techniques

2.2.1. Aerosol Mass Spectrometry

Two on-line aerosol mass spectrometers were used in the study and were housed in mobile laboratories parked within 25 m of the UK national air quality monitoring station (UK NAQS) and operated continuously from 19:00 h on 24th April 2006 to 13:00 h on 5th May 2006.

The aerosol mass spectrometers used were a TSI-ATOFMS (Model 3800-100, TSI, Inc.) and an HR-ToF-AMS (Aerodyne Research, Inc.). The ATOFMS (TSI Model 3800-100) collects bipolar mass spectra of individual aerosol particles. Briefly, particles are sampled through an orifice and accelerated through

the aerodynamic lens to the sizing region of the instrument. Here, the aerodynamic diameter of particles sizes between 100 nm and 3 μm is calculated based on their time of flight between two orthogonally positioned continuous wave lasers (λ = 532 nm). In terms of particle collection efficiency, this is a major improvement toward smaller particle sizes compared to the previous model of the ATOFMS (TSI Model 3800) that utilized a nozzle/skimmer interface for the inlet (Gard et al. 1997; Su et al. 2004). Particles are then transmitted to the mass spectrometry region of the instrument and the light scattered by the particles is used to trigger a pulsed high-power desorption and ionization laser (λ = 266 nm, 1 mJ pulse⁻¹) that desorbs and ionizes the particle in the centre of the ion source of a bipolar reflectron ToF-MS. Thus, positive and negative ion spectra of a single particle are obtained. The ATOFMS provides information on the abundance of different types of aerosol particles as a function of particle size with high time resolution (Su et al. 2004). ATOFMS can also provide chemical information if a relative sensitivity factor is applied (Gross, Galli, Silva, and Prather 2000; Dall'Osto and Harrison 2006) and methodologies are also available to convert ATOFMS data into continuous, semi-quantitative, and size-resolved mass concentrations, which can be used to provide a semi-quantitative estimate of the number and mass concentrations of particles from different sources (Dall'Osto and Harrison 2006; Qin et al. 2006). The TSI-ATOFMS data sets were imported into YAADA (Yet Another ATOFMS Data Analyzer) and single-particle mass spectra were grouped with adaptive resonance theory neural

TABLE 1
Brief summary of emission sources and types, and main components

Sector/plant	Plant/operation	Emission type	Components
<i>Ironmaking (230–270°C)</i>			
Sinter plant	Iron ore sintering	Stationary source – continuous	KCl, Fe, Pb, Zn, Mn
	Sinter plant de-dusting	Stationary source – continuous	Fe, Mn
Blast furnace	Tapping	Fugitive – intermittent	Fe, Mn
	Slag processing	Stationary source – intermittent	Ca, Al, Si, S
	Stove heating	Stationary source – continuous	CO ₂ , SO ₂ , NO _x
Raw materials	Unloading, stocking, blending wind entrainment	Fugitive – intermittent	Fe, Ca, Mg, Mn
<i>Steelmaking/cokemaking (190–230°C)</i>			
BOS plant	Steelmaking	Stationary source – batch	Fe, Zn, Pb, Mn
	Charging, blowing, tapping	Fugitive – intermittent	Fe, Zn, Pb, Mn
Cokemaking	Battery underfiring	Stationary source – continuous	CO ₂ , SO ₂ , NO _x , soot (C)
	Charging	Fugitive – intermittent	Organics, particulates
	Door and top leakages	Fugitive – intermittent	Organics, particulates
	Pushing	Fugitive – intermittent	Particulates
	Quenching	Fugitive – intermittent	Particulates, soluble salts
<i>Mills (160–190°C)</i>			
Rolling mills	Hot mill	Fugitive – intermittent	Fe, coolants
	Cold mill	Fugitive – intermittent	Lubricants, coolants

network, ART-2a (Song et al. 1999). The parameters used for ART-2a in this experiment were: learning rate 0.05, vigilance factor 0.85, and 20 iterations. Further details of the parameters can be found elsewhere (Dall'Osto and Harrison 2006; Rebotier and Prather 2007). An ART-2a area matrix (AM) of a particle cluster represents the average intensity for each m/z for all particles within a group. An ART-2a AM therefore reflects the typical mass spectra of the particles within a group.

The Aerodyne HR-ToF-AMS focuses aerosol particles in the size range 60–600 nm quantitatively onto a hot surface ($\sim 600^\circ\text{C}$) using an aerodynamic lens assembly. Smaller and larger particles are also collected, but with lower efficiency. Nonrefractory particle components flash-evaporate on the hot surface, the vapour that is produced is subjected to 70-eV electron impact ionization, and the resulting ions are transported into an orthogonal extraction time-of-flight mass spectrometer for high-resolution mass analysis. Particle size information is obtained by chopping the particle beam and collecting mass spectra as a function of particle flight time. During this field campaign, the instrument was operated in the low-resolution mode and provided 5-min averages of mass concentrations of the nonrefractory aerosol components as well as species-resolved size distributions. Due to the relatively low mass resolution of the AMS data, modern high-resolution analysis methods to separate individual components at certain nominal m/z cannot be applied. A detailed description of the instrument and its operation is given by Drewnick et al. (2005) and DeCarlo et al. (2006).

2.2.2. Other Instrumentation

In addition to the AMSs, a range of other on-line aerosol instruments were deployed to measure different physical characteristics of the ambient aerosols sampled. A multi-angle absorption photometer (MAAP, Thermo Electron) was used to measure 1-min averages of the ambient $\text{PM}_{1.0}$ black carbon (BC) concentrations. In addition to the aerosol instruments, a mobile meteorological station was operated at a distance of approximately 10 m, providing 1-min averages of all relevant meteorological parameters.

3. RESULTS

3.1. General Meteorological and Air Quality Parameters During the Field Study

Five-day back-trajectories of the air masses arriving at the measurement site were calculated for 00:00 h and 12:00 h for each day of the campaign by the British Atmospheric Data Centre. The predominant origin of air masses arriving at the receptor was westerly, with Atlantic air masses not strongly influenced by anthropogenic pollution. On a few occasions, air masses had previously traveled over inland industrialized regions. The weather during the field study was characterized by unusually warm seasonal conditions (temperature $11.5 \pm 3.1^\circ\text{C}$, relative humidity $72.8 \pm 12.7\%$; 1 SD of hourly data) and very low rainfall (only two small events within two weeks). Furthermore,

wind speed was generally low (average during the field study $1.3 \pm 1.0 \text{ m s}^{-1}$), with very few occasions of higher wind speeds ($>6 \text{ m s}^{-1}$). The local wind pattern was characterized on some days by a typical sea-breeze pattern, with wind from the land to the sea in the late night and in the opposite direction during the afternoon. The average of hourly PM_{10} data recorded by the UK monitoring site at Port Talbot throughout the entire campaign was $33 \pm 22 \mu\text{g m}^{-3}$ (SD), while the average daily concentration was $33 \pm 8 \mu\text{g m}^{-3}$. The 24-h limit value for PM_{10} was not exceeded during any day of the campaign.

3.2. Particle Mass Spectrometry

The TSI-ATOFMS sized about 4.7 million particles, of which approximately 535,000 particles were ionized, and the ART-2a algorithm used about 95% of these data in generating 507 clusters to describe the data set. By manually merging similar clusters (Dall'Osto and Harrison 2006), the total number of clusters describing the whole database was reduced to 30. The main features of particle types attributed to the nearby steelworks were sharp and relatively intense spikes of particulate matter detected from the wind sector $160\text{--}300^\circ$ (Figure 1). These particle types were seen mainly as intense spikes and were not found in the background air. Common particle types (Table 2, others, 68.4%) including sea salt, soil dust, biomass burning, and lubricating oil were ascribed to other sources, i.e., originating from natural sources, the motorway, and the nearby town of Port Talbot. Most of these particle types have already been described in the literature (Liu et al. 2003; Pastor et al. 2003; Dall'Osto and Harrison 2006) and will not be further discussed here. Of the total particles classified, 32% were apportioned to the steel industry: nonmetallic particle types (eight TSI-ATOFMS classes in total) constituted 27% of the particles, while "metal-rich" types contributed 4.5% of the total (Dall'Osto et al. 2008). During this field campaign (Dall'Osto et al. 2008, this study), the ATOFMS provided information on the mixing state of the aerosols detected. Most of the particle types contained both organic and inorganic species, including alkali and trace metals. While nonmetallic particles (this study) also contain some traces of both inorganic species (nitrate, sulfate) and some metals (Na, K), the main feature is

TABLE 2
Summary of the main ATOFMS classes obtained using ART-2a, detected during spring 2006, Port Talbot

ATOFMS particle types	Number of subclasses	<i>N</i> particles	%
Metal-containing particles from steelworks (Dall'Osto et al. 2008)	6	17,967	4.5
Nonmetal-containing particles from steelworks (this study)	8	108,731	27.0
Others	16	274,109	68.5
Total	30	400,807	100.0

represented by organic and sulfur signatures (in this context elemental carbon [EC], organic carbon [OC], and sulfur).

3.3. Steelworks-Related Particle Types

As discussed in the following sections, the positive- and negative-ion ART2a area matrices of each cluster were unique. However, some of the temporal trends of the eight ATOFMS clusters were very similar ($R^2 > 0.85$) to each other, which is likely to be due to some of the particle types sharing a common source or source process. TSI-ATOFMS classes with similar temporal trends were summarized into three main groups of particles, as shown in Table 3.

These groups were characterized by very sharp temporal trends of increased particulate mass concentrations (up to $140 \mu\text{g m}^{-3}$ of PM_{10}) owing to aerosol releases from the steelworks. Analysis of meteorological data associated these three groups with three distinct wind sectors, being $230\text{--}260^\circ$ for group 1,

$190\text{--}230^\circ$ for group 2, and $160\text{--}190^\circ$ for group 3. The three wind sectors of the respective groups of particle release events were different from each other. However, within a given wind sector, several potential sources of aerosol emission exist, as can be seen in Figure 1. The main emission sources are the sinter plant and blast furnace in sector 1 (denoted ironmaking); BOS and coke ovens (CO) in sector 2 (named steel/cokemaking) and the hot and cold rolling mills in sector 3 (referred to as mills). Furthermore, within each of these sectors, there are other nonspecific sources arising from general movement of traffic and from the handling and storage of particulate materials on site. Aerosol sampling times characterized by at least 75% of the total classified TSI-ATOFMS particle mass spectra belonging to a single-source sector-related particle group (Table 2) were classified as steelworks' particle events. In other words, not more than 25% of the particles detected by the ATOFMS could be attributed to nonsteel sources during the steelworks particle events.

TABLE 3

Summary of ART-2a subclasses associated with nonmetallic steel industry sources. Wind roses were calculated with the main particle type belonging to each steelworks process. Minor ATOFMS particle types belonging to the same group gave very similar wind roses

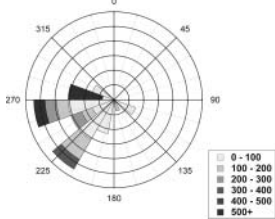
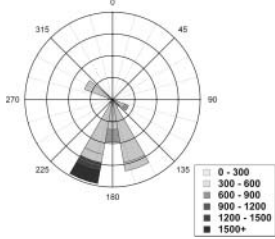
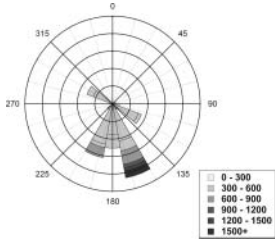
Main ATOFMS particle group	ATOFMS subclass names	Size (scaled ATOFMS aerodynamic diameter)	Wind rose	Main chemical components	% of the total
1	Sulfur	350 nm		Elemental sulfur, traces of organics	2.7
2	EC-OC-Sul	300 nm		Elemental carbon, organic carbon, sulfate	6.6
	Nit-Sul	400 nm		Nitrate, sulfate	3.9
	PAH_high	<250 nm		PAHs with high molecular weight	2.1
3	Aro-CN	300 nm		Aromatic and nitrogen-containing carbon compounds	8.0
	CN-Sul	450 nm		Nitrogen-containing carbon compounds, sulfate	1.8
	PAH_low	<250 nm		PAHs with low molecular weight	1.4
	HOC-Cl	300 nm		High molecular weight organic carbon, chloride	0.6

TABLE 4
Summary of averaged real-time aerosol and gas measurements detected during periods of events of main ATOFMS particle groups 1–3

Main class	1	2	3
Wind sector	230–260°	190–230°	160–190°
<i>Sector-related steelworks processes</i>	<i>Ironmaking</i>	<i>Steel/cokemaking</i>	<i>Mills</i>
Black carbon ($\mu\text{g m}^{-3}$)	0.74	1.1	0.66
ToF-AMS sulfate ($\mu\text{g m}^{-3}$)	3.2	4.5	2.1
ToF-AMS nitrate ($\mu\text{g m}^{-3}$)	0.15	1.1	0.22
ToF-AMS ammonium ($\mu\text{g m}^{-3}$)	0.65	1.6	0.58
ToF-AMS organics ($\mu\text{g m}^{-3}$)	0.87	2.4	1.1
ToF-AMS chloride ($\mu\text{g m}^{-3}$)	0.12	0.6	0.09
ToF-AMS PAHs ($\mu\text{g m}^{-3}$)	0.003	0.14	0.009
ToF-AMS organics/black carbon	1.18	2.27	1.69

Moreover, it is important to remember that the average PM_{10} concentrations during those events were always about 2–4 times higher than the background aerosol mass concentrations. For these time intervals, average concentrations, derived from the HR-ToF-AMS and MAAP, are summarized in Table 4. The aerosol characteristics associated with the three sectors are presented in the following sections, with a discussion of the likely steelworks sources. The HR-ToF-AMS and MAAP data are influenced by background aerosol, but as is clear from Figure 1, the site location is such that within the three defined sectors, the instrument sampled air that had approached over the sea from the south and west before crossing the steelworks en route to the air sampling site. The easterly sectors associated with a high regional background (Harrison et al. forthcoming) were not included.

3.3.1. Sector 1 (Ironmaking)

This sector contains two major steelworks' processes, the sinter plant (SP) and the blast furnace (BF) (Figure 1). Other activities associated with this sector include the unloading of iron ores and coals at the wharf, stocking of raw materials, and the blending of raw materials preparatory to their use in the sinter plant. Figure 2a shows the ART-2a AMs of a particle type denoted "sulfur," which is the only TSI-ATOFMS nonmetallic particle type characterizing this sector. Peaks at m/z 32 [S], 64 [S_2], 96 [S_3], 128 [S_4] and 160 [S_5] can be seen in both positive- and negative-ion mass spectra, indicating the strong presence of sulfur. With regard to the mixing state of this sulfur-rich TSI-ATOFMS particle type, peaks at m/z 27 and 29 (C_2H_3^+ and C_2H_5^+ , respectively) could be seen at very low intensities. Insofar as is known, this ATOFMS particle type has never been reported previously in the literature. It is important to note that the detection of this particle type coincided with the olfactory detection of a noticeable sulfurous odour by scientists involved in the monitoring campaign, which was considered likely to be due to the presence of hydrogen sulfide (H_2S) in the air

(Campagna et al. 2004). Hydrogen sulfide is often present in emissions from petrochemical refineries, pulp and paper industry, gasworks, wastewater and biogas plants, coking plants, and blast furnaces. The temporal trend of the ATOFMS detection rate for this particle type, showing specific spikes, is shown in Figure 3a, where a distinct event (1 June 2006 15:00–19:00 h) can be seen. Gas phase SO_2 (taken from UK NAQS data) also

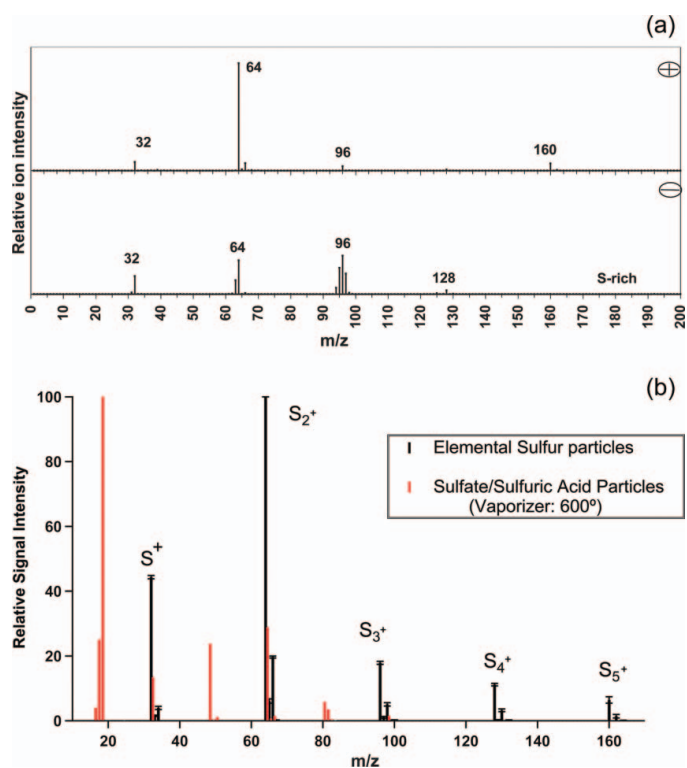


FIG. 2. (a) Positive (+) and negative (-) ART-2a area matrices attributed to TSI-ATOFMS cluster sulfur. (b) Averaged HR-ToF-AMS single m/z resolution mass spectrum for the sulfur aerosol components. (Color figure available online).

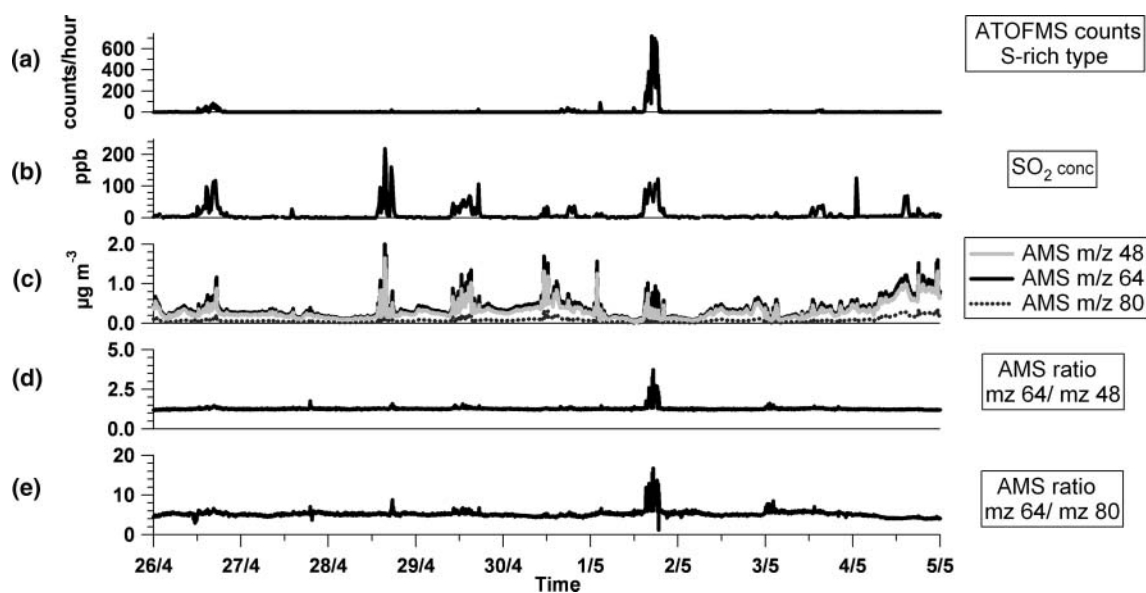


FIG. 3. Time series of various aerosol and gas parameters for the whole field study: (a) 10-min TSI-ATOFMS temporal trends for S-sulfur particle type, (b) SO_2 concentrations (ppb), (c) 5-min temporal trends for specific m/z 48, 64, and 80 by HR-ToF-AMS, and (d) HR-ToF-AMS ratio m/z 64/48 and (e) HR-ToF-AMS ratio m/z 64/80.

exhibited a spike (about 70 ppb – Figure 3b) during the same period.

The HR-ToF-AMS data support the TSI-ATOFMS findings. Common main ion fragments used to identify sulfate and sulfuric acid aerosol species in HR-ToF-AMS spectra are m/z 48 [SO^+], 64 [SO_2^+], 80 [SO_3^+], 81 [HSO_3^+], and 98 [H_2SO_4^+] (Canagaratna et al. 2007). For these species, a typical fragmentation pattern is observed with m/z 48 and m/z 64 peaks having similar intensity and with the signal at m/z 80 being approximately five times less intense than at the m/z 64 peak. In Figure 3c, the temporal trends in the mass concentrations of these three sulfate-related m/z species are shown. While they exhibit very similar trends during the whole measurement period, the ratios between the signals at m/z 64 and 48 (Figure 3d) and between the signals at m/z 64 and 80 (Figure 3e) show clear variations that are correlated both with the peaks of TSI-ATOFMS sulfur particle type counts and the SO_2 concentration obtained from the UK NAQS. Whenever the sulfur type of particle was detected with higher count rates, the ratio of m/z 64 signal to those of the two mentioned sulfate-related signals increased in the HR-ToF-AMS mass spectra.

In order to explain this behavior, laboratory experiments were performed with the HR-ToF-AMS, wherein pure sulfur particles were generated by evaporation and re-condensation of elemental sulfur in an argon atmosphere and then characterized with the AMS. From these measurements, the standard fragmentation pattern of elemental sulfur particles shown in Figure 2b (black bars) was extracted. These spectra show that such particles generate signals at m/z 32 [S^+], 64 [S_2^+], 96 [S_3^+], $n \cdot 32$ [S_n^+], and at the related isotope m/z values. No signals were found at m/z 48 or 80 in contrast to the fragmentation patterns of sulfate

or sulfuric acid (red bars in Figure 2b). Therefore, the sharp and strong increase in the m/z 64/48 and m/z 64/80 signal ratios observed during the measurement of the sulfur particles with the TSI-ATOFMS is a good indication that the HR-ToF-AMS also measured elemental sulfur particles, which generate a signal at m/z 64 but not at m/z 48 or 80, during these time intervals. This also represents the first time that such a particle type has been observed with an HR-ToF-AMS.

Figure 4a shows the HR-ToF-AMS-averaged aerosol size distributions for the period dominated by the ATOFMS sulfur particle type. Besides the accumulation mode, likely to be due to the background aerosol, a unique ‘sulfate’ mode can be clearly seen at about 80 nm. It is important to note that this aerosol component commonly classified as ‘sulfate’ in the standard HR-ToF-AMS data processing in our samples is in reality composed of elemental sulfur.

This unique particle type is most likely to have originated from slag processing at the blast furnaces, where both open-pit cooling and slag granulation are carried out. Most of the slag from the blast furnace (85–90%) is granulated, wherein the slag stream is cooled rapidly with water, producing slag granules that are used in cement manufacture. The gases from this process (mainly steam) are emitted to atmosphere via a short stack. In open-pit practice, the slag is run into a large rectangular pit, where it is allowed to cool in air and then quenched using water sprays. During the period of air cooling, sulfur dioxide is released slowly by oxidation of sulfur in the slag with atmospheric oxygen, but during water quenching, hydrogen sulfide is formed in larger amounts than sulfur dioxide. When the pit is full, the slag is removed as a solid massy product, using heavy duty diggers, and taken to a slag processing plant. In both

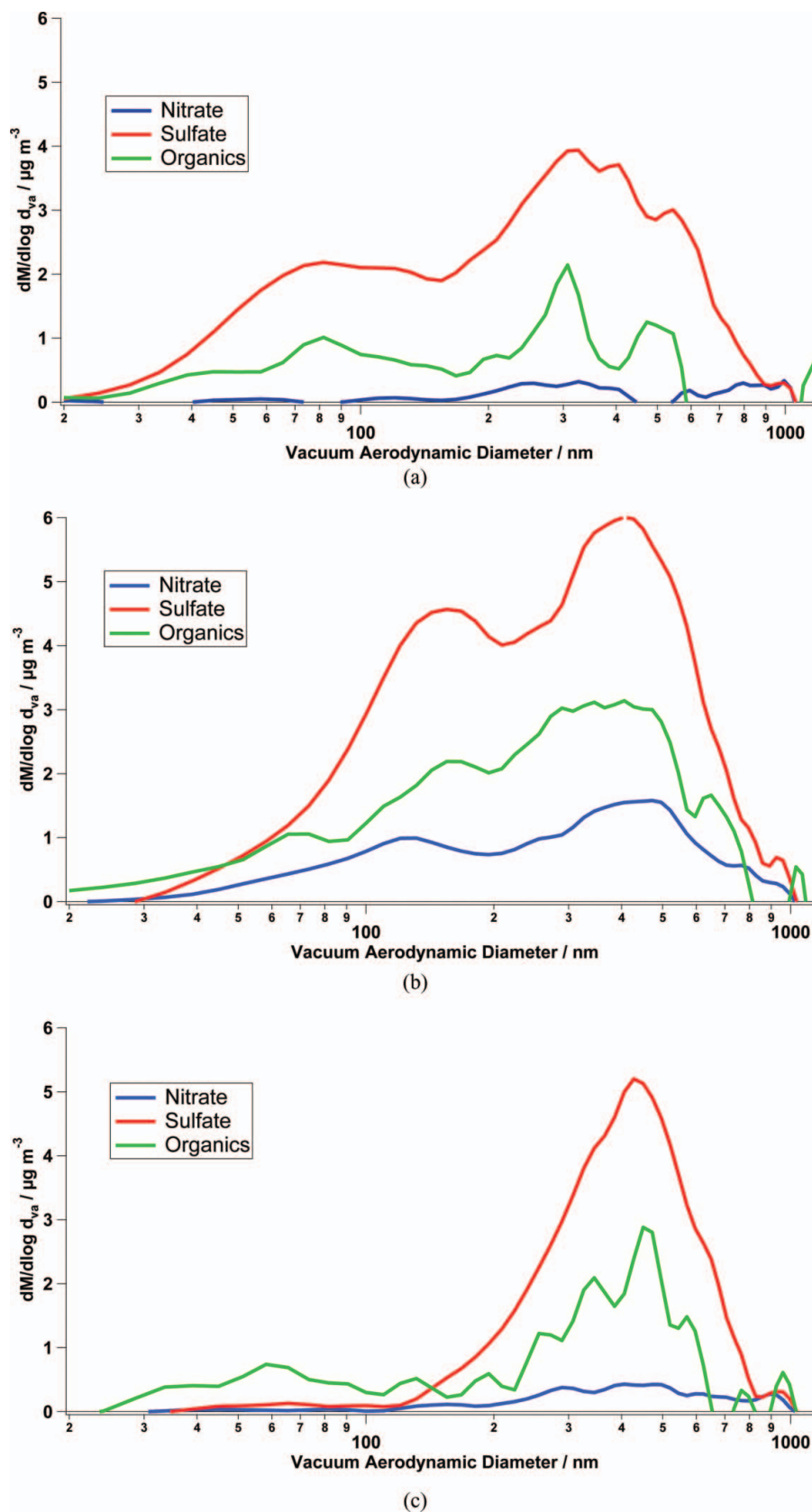


FIG. 4. HR-ToF-AMS aerosol size distributions for nitrate, sulfate, and total organics for events characterized by (a) S-sulfur, (b) Aro-CN, and (c) EC-OC-Sul TSI-ATOFMS particle types. (Color figure available online).

processes, hydrogen sulfide is produced during water quenching, which explains the olfactory detection of hydrogen sulfide. Technically, it is possible for sulfur particles to be released from either slag granulation or open-pit slag operation and further studies would be required to establish unequivocally the main source of such particles. It is known that both slag granulation and the digging out of an open pit took place during the time in question but the plant records are not sufficiently precise to enable the source to be more definitely apportioned. Laboratory studies by Agrawal et al. (1983) reported the kinetics and mechanism of the desulfurization of liquid blast furnace slag and the rate of evolution of sulfur-bearing gases. It was concluded that the sulfur-bearing species evolved from the surface of the slag was S_2 when the rate was second order with respect to the concentration of adsorbed sulfur ions, but SO_2 was evolved when the rate was first order with respect to the concentrations of adsorbed sulfur ions. Insofar as is known, the present study confirms for the first time the presence of elemental sulfur particles in the atmosphere, formed at high temperature in the blast furnaces and emitted together with H_2S .

3.3.2. Sector 2 (Steel/Cokemaking)

TSI-ATOFMS particle types associated with this sector were mainly detected when the wind was blowing from the $190\text{--}230^\circ$ direction, where the basic oxygen steelmaking (BOS) and coke oven (CO) plants are located. The coke ovens are considered one of the main sources of carbon-containing particulate matter in the steelworks (Khalili et al. 1995; Yang et al. 2002; Jiun-Hong et al. 2007). In the coke ovens, blended coals are charged to a series of slot ovens and heated to approximately $1250\text{--}1300^\circ\text{C}$ for 18–20 h, after which the product coke is pushed into a car and transported a short distance by rail to a quenching tower, where the coke is cooled rapidly (60–90 s) by spraying with water. There are 84 coke ovens at Port Talbot and these are charged and pushed according to a defined sequence so that although cokemaking is a batch process, there is regularity of operation and, consequently, of emissions resulting from the different activities.

In the BOS plant, liquid iron from the blast furnaces is transferred into converter vessels and refined into liquid steel by blowing pure oxygen onto the surface of the molten bath. The BOS process is also operated batch wise, with each charge of approximately 340 tonnes of steel scrap and liquid iron taking approximately 35–40 min to process. Typically, there are two converters operating in parallel so that again there is a high degree of regularity in the processes, which may lead to particulate emissions. Episodic events in PM_{10} concentrations associated with the BOS plant were mainly composed of metal-rich particles (Dall'Osto et al. 2008).

The ART-2a positive and negative aerosol masses of the major TSI-ATOFMS cluster related to this sector (EC-OC-Sul, about 50% of the particles belonging to group 2) are shown in Figure 5a. A strong OC signature can be seen at m/z 36 [C_3^+], 37 [C_3H^+], and 38 [$C_3H_2^+$] and the same signature is also seen

at m/z 48 and 60. The m/z range above 100 shows only an EC signature at m/z 108, 120, 132, and 144 [C_n^+ , $n = 9\text{--}12$]. No indications of other signals due to high-MW compounds can be seen. Finally, the negative-ion spectrum shows a strong sulfate peak at m/z -97 [HSO_4^-], with a weak signal at m/z -26 [CN^-]. The second-most abundant cluster for this sector was named Sul-Nit (Figure 6a, 30% of the particles of this sector), reflecting the presence of nitrate (m/z at -46 and -62) and sulfate (m/z -97). This cluster is represented only by a negative AM, similar to cluster EC-OC-Sul, with a complete absence of any peak in the positive AM. The temporal correlation between cluster EC-OC-Sul and Sul-Nit was very high ($R^2 > 0.95$), and it is likely that these two classes are from sources in close proximity. While cluster EC-OC-Sul showed a size distribution peaking at 300 nm, cluster Sul-Nit peaked at 400 nm. Moreover, the nitrate signal of cluster Sul-Nit is more intense than the one of cluster EC-OC-Sul. The slightly coarser mode of cluster Sul-Nit, relative to the EC-OC-Sul one, is likely to be due to the presence of nitrate. Both particle types are attributed to the coke oven combustion processes. Quantitative results from other instruments support the TSI-ATOFMS findings characterizing this sector. First, the HR-ToF-AMS detected the highest concentration of organic aerosol species ($2.4 \mu\text{g m}^{-3}$) in comparison to the other two sectors, consistent with the strong OC signature of cluster EC-OC-Sul (Table 4). Also, in agreement with this strong particle type, the PM_{10} EC content was also found to be highest ($1.1 \mu\text{g m}^{-3}$). The ratio HR-ToF-AMS organics/MAAP EC was 2.27, the highest of the three particle groups, supporting the strong OC signature of the ATOFMS mass spectra. The nitrate signature found mainly in TSI-ATOFMS particle types from this sector is in agreement with the highest HR-ToF-AMS nitrate aerosol loading ($1.1 \mu\text{g m}^{-3}$) among the three sectors.

Figure 4b confirms the presence of a small-particle mode ($d_{va} \sim 150$ nm) aerosol with internally mixed organics, nitrate, and sulfate, as found in the EC-OC-Sul and Sul-Nit particle types. The high HR-ToF-AMS sulfate loading for this sector ($4.5 \mu\text{g m}^{-3}$) also reflects the strong sulfate signature found in the particle types from sector 2, which is southwesterly and unlikely to be influenced appreciably by regional transport sources.

Two types of PAH-containing particles types were detected with the ATOFMS, one of which was found mainly in this sector. The ART-2a area matrices of cluster PAH.highMW are shown in Figure 6c. This exhibits strong signals at m/z 202, 228, 252, 276, and 278, which could be associated with the presence of benzopyrene and/or benzofluoranthene in the particles (Gross, Galli, Silva, Wood et al. 2000). PAH detection with the HR-ToF-AMS has been previously reported (Dzepina et al. 2007). Using ATOFMS time series of PAH-containing particles, time intervals with different PAH-related features were determined. For deeper analysis of the AMS PAH data, not all PAH-related signals from the organics mass spectra were summed to calculate a total PAH concentration, but the low- and high- m/z signals were treated separately. Thus, two different classes of PAH

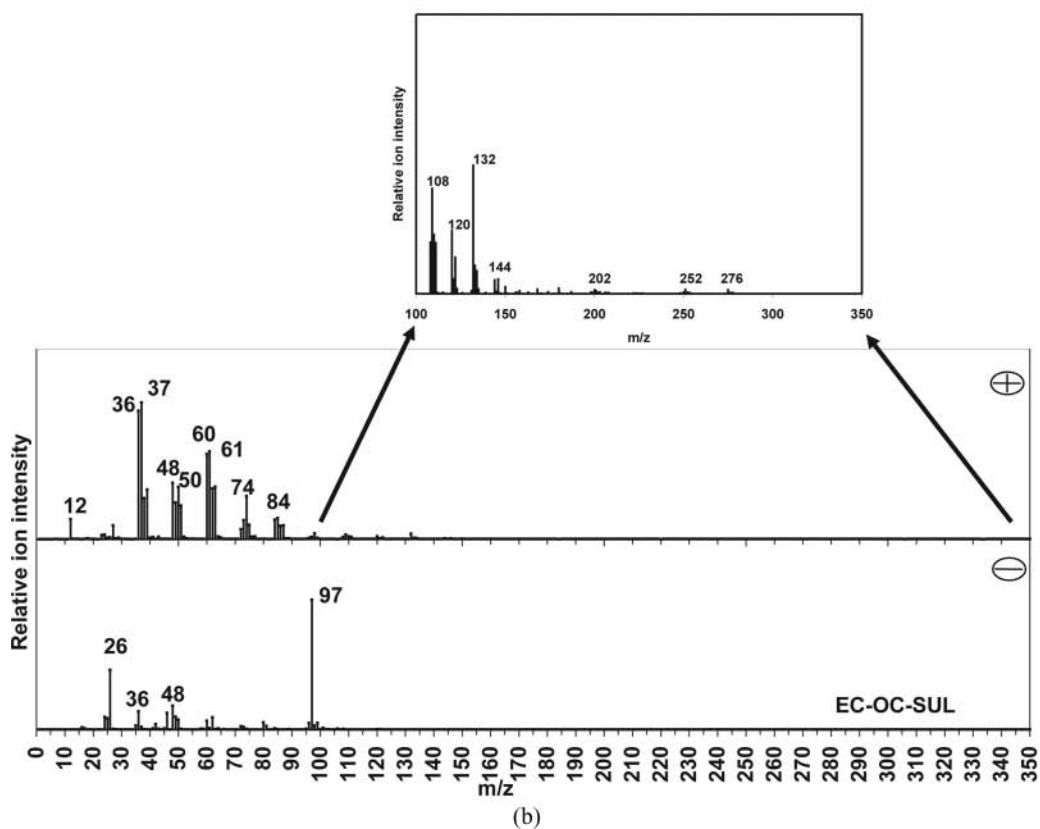
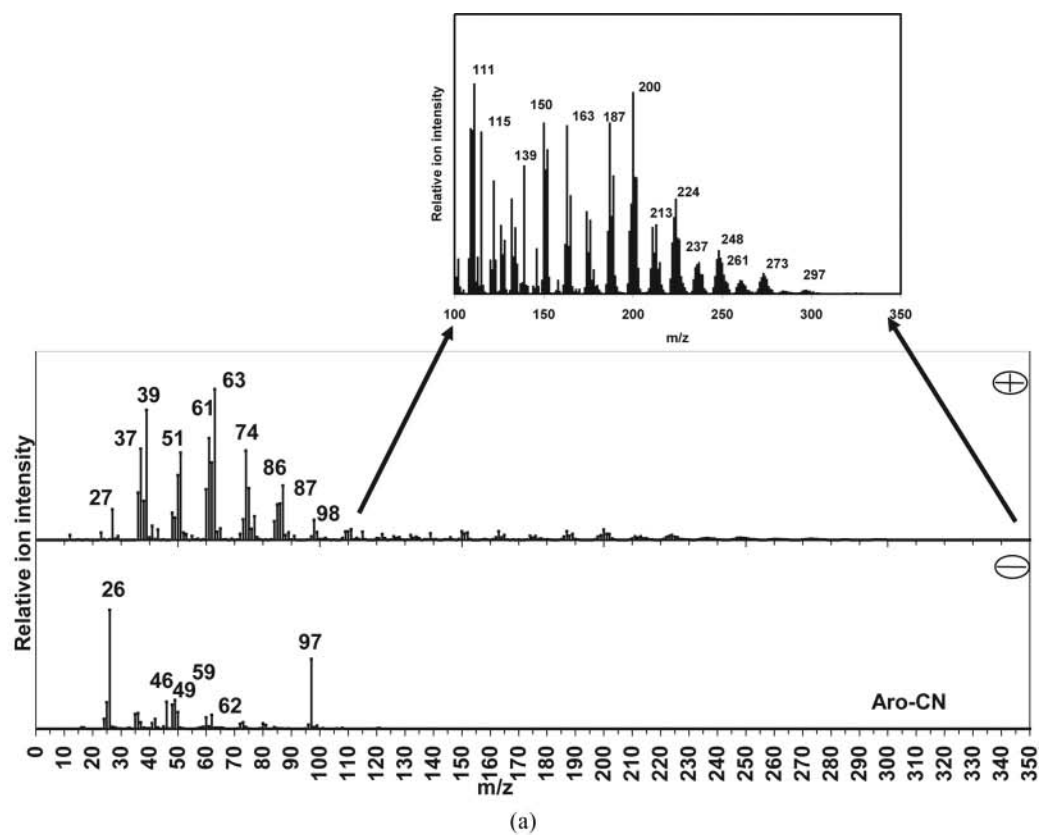


FIG. 5. Positive (+) and negative (-) ART-2a area matrices attributed to (a) EC-OC-Sul and (b) Aro-CN.

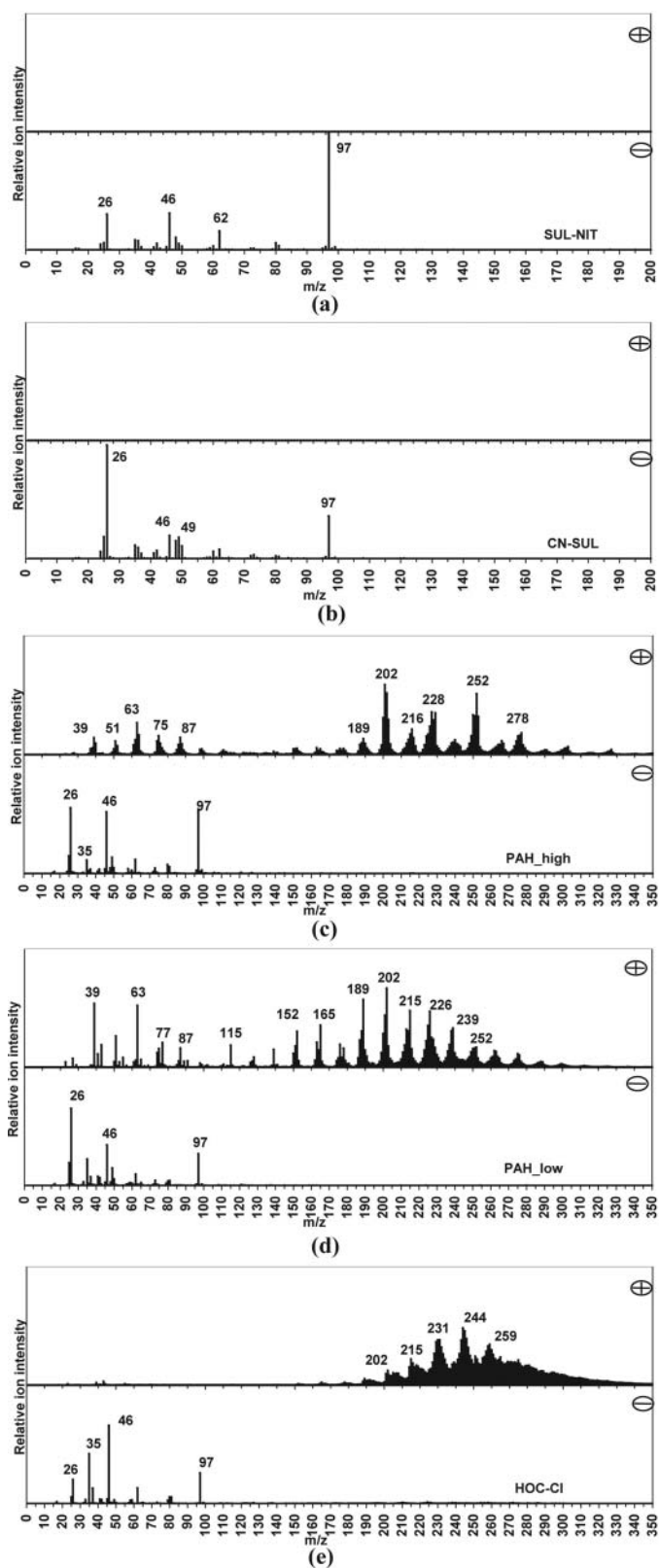


FIG. 6. Positive (+) and negative (-) ART-2a area matrices attributed to (a) PAH_low, (b) PAH_high, (c) CN-Sul, (d) Sul-Nit, and (e) HOC-Cl.

(high- and low-MW PAH) were found within the AMS data set of this field campaign. The preliminary AMS analysis supports the ATOFMS findings by showing mass spectra with signals due to PAHs with high MW during the times when these particle types were detected. Coke oven emissions are known for having strong PAH signatures (Khalili et al. 1995; Yang et al. 2002; Jiun-Hong et al. 2007) and the PAH mass loading determined by the HR-ToF-AMS from sector 2 ($0.14 \mu\text{g m}^{-3}$) was more than one order of magnitude higher than that from the other sectors.

3.3.3. Sector 3 (Mills)

This sector named “Mills” contains processes such as the hot and cold mills (Figure 1). The metallurgical process of hot rolling is used to produce finished or semi-finished steel products such as steel strip (the main product at Port Talbot), beams, angles, rails, billets, bars, etc., by deforming steel between a set of work rolls above its re-crystallization temperature. Cold rolling is used mainly for final processing of strip products and takes place below the re-crystallization temperature of the steel. Table 3 shows four TSI-ATOFMS particle types associated with sector 3: Aro-CN, CN-Sul, PAH_low, and HOC-Cl. The main cluster (70% of the TSI-ATOFMS mass spectra belonging to this particle group, 8% of the total classified during this field study) is represented by the Aro-CN particle type. This particle type was found to be rich in aromatic and nitrogen-containing compounds, as shown in the AMs in Figure 5b. Signals due to the aromatic series appear at m/z 51 [C_4H_3^+], 63 [C_5H_3^+], 77 [C_6H_5^+], and 91 [C_7H_7^+] (Liu et al. 2003). Strong peaks at m/z 74 [diethylamine $\text{C}_4\text{H}_{11}\text{N}^+$] and m/z 86 [$(\text{C}_2\text{H}_5)_2\text{N} = \text{CH}_2^+$] are attributed to organic nitrogen-containing compounds (Angelino et al. 2001; Moffet et al. 2004). The presence of a peak at m/z -26 [CN^-] confirms the presence of organic nitrogen-containing compounds also in the negative-ion spectrum. The presence of a peak at m/z 39 is often associated with potassium [K^+], but it could also be due to an organic fragment [C_3H_3^+] (Silva and Prather 2000). A closer examination of the positive-ion mass spectrum of this class shows many more peaks at m/z above 100. Signals at m/z 115, 139, 150, 163, 187, 200, 213, 224, 226, 248, 261, 273, and 297 can be seen in the positive ART2a AMs. Definitive assignments for these high- m/z peaks (m/z above 100) are difficult to make a priori since more than one possibility exists for each m/z value. However, the unidentified m/z signals are not associated with PAHs or other high ATOFMS m/z previously reported (Silva and Prather 2000; Qin and Prather 2006; Denkenberger et al. 2007).

The cluster CN-Sul (Figure 6b) is the second-most abundant ATOFMS particle type belonging to group 3, containing about 15% of the particles of this group. It is characterized only by a negative-ion mass spectrum, very similar to that for the cluster Aro-CN (Figure 5b). No indication of a positive-ion mass spectrum was found to be associated with any particle within this cluster. In addition, the temporal correlation between the two classes was very high ($R^2 > 0.98$). Therefore, it is likely

that these two classes represent the same particle type. The difference is likely to be due to shot-to-shot variations of the ATOFMS LDI laser that can generate different mass spectra for the same particle type (Gross, Galli, Silva, and Prather 2000). In this case, some particles of these types were hit by the LDI laser pulse, but only negative-ion mass spectra were generated. However, while the scaled TSI-ATOFMS size distributions for class Aro-CN peaked in the smallest ATOFMS detection size (300 nm), cluster CN-Sul peaked at 450 nm.

Air emissions from hot mills may include stationary-source emissions of gases and particles generated by the combustion of fuel in the reheating furnaces as well as fugitive releases of volatile organic compounds (VOCs) and nitrogen gases from cold rolling and lubrication oils. Moreover, water treatment is widely required in the mills processes. The results suggest that nitrogen-containing organic aerosol is characteristic of the PM emitted from this sector. The origin of the nitrogen signature in the mills sector is difficult to explain but possibly may be due to nitrogen-containing compounds (such as ammonia) used in water treatment chemicals.

A second TSI-ATOFMS PAH particle type (PAH_{lowMW}, Figure 6d) was detected during the field study and was apportioned to particle group 3. Signals at m/z 189, 202, 216, and 226 are likely to be due to low-MW PAHs. The signal at m/z 202 is likely to arise from pyrene and/or fluoranthene (Gross, Galli, Silva, Wood et al. 2000).

The AMs of ART-2a cluster HOC-Cl (Figure 6e, 5% of the particles belonging to group 3) exhibit a positive-ion mass spectrum, with intense signals being distributed above m/z 200, including major unidentified peaks at m/z 231, 244, and 259. Again, the peaks at m/z -26 and -46 indicate a nitrogen signature. Moreover, the presence of strong signals at m/z -35 and -37 [Cl^-], not seen in the other particle types, suggest that this particle type is the only one internally mixed with chloride. Hydrochloric acid pickling is used in the tandem cold mill (TCM) process and thus could be a source of this particle type. This "Mills" sector exhibited the lowest BC concentration ($0.66 \mu\text{g m}^{-3}$) among all three sectors, consistent with the absence of EC signatures in the ATOFMS clusters. Figure 4c shows the average HR-ToF-AMS size distribution, exhibiting a smaller particle size mode of organic aerosol likely to be associated with the fine ATOFMS particle types of sector 3.

4. DISCUSSION

Emissions from stationary sources are generally well characterized because they can be sampled using well-validated or standard methods. However, there are numerous fugitive sources on an integrated steelworks that are less well characterized. These often involve episodic events and may include area sources, such as stockyards, fugitive process emissions, the movement of materials around the works, or traffic on works' roads. In order to address the problems of particulate fugitive

releases, the UK steel industry is carrying out major research investigations in order to identify the main sources so that investments to control releases can be targeted toward the most important sources.

The work reported here forms part of the overall work that is being carried out to improve the steel industry's understanding of the generation and dispersion of fugitive emissions. In this study, the application is described of two different types of aerosol mass spectrometer, namely a TSI-ATOFMS (Model 3800-100, TSI, Inc.) and a HR-ToF-AMS (Aerodyne Research, Inc.), to characterize particles in ambient air in the surroundings of a major integrated steelmaking plant in the UK. The results demonstrate the power of these state-of-the-art techniques for probing the chemical composition of particulate matter in ambient air and reveal some novel information on nonmetallic particle types associated with steelworks' emissions. Table 5 summarizes the finding of this study as well as that of Dall'Osto et al. (2008), providing overall the main results of this field study, where co-located ATOFMS, AMS, MOUDI, and MAAP measurements were taken. Three main ATOFMS groups of particle types were associated with different sectors. For each of those, average mass concentrations were provided by the MAAP and the AMS. Moreover, three of the nine MOUDI samples were strongly influenced by the emissions of selected parts of the largest integrated steelworks in the UK.

Elemental sulfur species, likely to be released in slag processing operations associated with the blast furnace, were reported for the first time in the aerosol phase by both the TSI-ATOFMS and the HR-ToF-AMS. However, it was not possible to determine the extent to which the sulfur species were released by slag granulation and open-pit practices. Additional studies next to the processing operation should be carried out to further elucidate the mechanisms. Furthermore, Fe-rich particles were detected by the ATOFMS from this ironmaking sector, confirmed by high mass loadings of Fe (and Mn) sampled with a MOUDI and found to be unimodally distributed at $6 \mu\text{m}$. The coarse unimodal distribution observed from this ironmaking sector indicates that wind-entrained dust from the iron ore stockpiles is likely to be the major source. In contrast, the ATOFMS data analysis showed that the steelmaking/cokemaking processes were associated with the elevated particle number concentrations rich in OC, EC, nitrate, sulfate, and PAH with high MW. The AMS supports the ATOFMS findings with the highest aerosol mass loadings of the three steelworks sectors and the presence of small-particle mode (about 150 nm) aerosol with internally mixed organics, sulfate, and nitrate. This sector presented inorganic particles rich in Fe and Zn, but it was the least characterized in terms of metallic species. Finally, nitrogen-containing organic species, aromatic compounds, and PAH with low MW were related to the sector containing the hot and cold rolling mills, and perhaps related to VOC emissions associated with these processes and from water treatment activities. This sector was characterized by the lowest BC concentrations of all three steelworks sectors, but presented organic

TABLE 5
Summary of ATOFMS, AMS, MAAP, and MOUDI co-located measurements

	This study			Dall'Osto et al. (2008)	
	ATOFMS nonmetallic particle types	HR-ToF-AMS aerosol mass loadings	MAAP BC mass concentrations	ATOFMS metallic particle types	MOUDI
Ironmaking	Sulfur	Unique sulfur signal with a sulfate mode at 80 nm	$0.74 \mu\text{g m}^{-3}$	Fe	Fe, Mn unimodally distributed at $6 \mu\text{m}$
Steel/coke	EC-OC-Sul, Nit-Sul, PAH.HighMW	High aerosol mass loadings, mode at 150 nm internally mixed with Sul, Nit, and OC	$1.10 \mu\text{g m}^{-3}$ (highest loadings)	Zn	Fe-Pb at $0.45 \mu\text{m}$; Pb, Zn, K, and Cl at $1.2 \mu\text{m}$; and Fe, P, and Ca at $4 \mu\text{m}$
Mills	Aro-CN, CN-Sul, PAH.LowM, HOC-Cl	Fine organic mass in the sub 100-nm sizes	$0.66 \mu\text{g m}^{-3}$	Ni, Pb, KCl, FeP, Zn	Fe-Pb at $0.45 \mu\text{m}$; Pb, Zn, K, and Cl at $1.2 \mu\text{m}$; and Fe, P, and Ca at $4 \mu\text{m}$

aerosol concentrations distributed in the sub-100-nm mode. This sector was also found to be characterized by a number of peculiar particles with high metal content. The ATOFMS revealed a number of unique particle types, including Ni, Pb, KCl, FeP, and Zn particle types. The MOUDI results were consistent with the variety of metal-rich particle types detected with the ATOFMS: a mode at $0.45 \mu\text{m}$ with Fe and Pb; a mode at $1.2 \mu\text{m}$ with Pb, Zn, K, and Cl; and a mode at $4 \mu\text{m}$ with Fe, P, and Ca.

The results presented in this paper show that the synergy of quantitative aerosol particle ensemble mass spectrometry (HR-ToF-AMS), single-particle mass spectrometry (ATOFMS), and an off-line filter technique (MOUDI) provides valuable highly complementary information about the nature of different aerosol sources. Together, they provide a valuable insight into the composition and the size distributions of both sub- and super-micron aerosol emissions from the steel industry. These signatures can potentially be used for detecting steelworks emissions at regional level.

REFERENCES

- Agrawal, B., Yurek, G. J., and Elliott, J. F. (1983). Kinetics and Mechanism of the Desulfurization of Liquid Blast-Furnace Slags by Ar-H₂O Gas Mixtures. *Met. Trans. B Process Metall.*, 14:221–230.
- Anderson, D. R., and Fisher, R. (2002). Sources of Dioxins in the United Kingdom: The Steel Industry and Other Sources. *Chemosphere*, 46:371–381.
- Angelino, S., Suess, D. T., and Prather, K. A. (2001). Formation of Aerosol Particles from Reactions of Secondary and Tertiary Alkylamines: Characterization by Aerosol Time-of-Flight Mass Spectrometry. *Environ. Sci. Technol.*, 35:3130–3138.
- Aries, E., Anderson, D. R., Fisher, R., Fray, T. A. T., and Hemfrey, D. (2006). PCDD/F and “Dioxin-Like” PCB Emissions from Iron Ore Sintering Plants in the UK. *Chemosphere*, 65:1470–1480.
- Campagna, D., Kathman, S. J., Pierson, R., Inserra, S. G., Phifer, B. L., Middleton, D. C., et al. (2004). Ambient Hydrogen Sulfide, Total Reduced Sulfur, and Hospital Visits for Respiratory Diseases in Northeast Nebraska, 1998–2000. *J. Exp. Anal. Environ. Epidemiol.*, 14:180–187.
- Canagaratna, M. R., Jayne, J. T., Jimenez, J. L., Allan, J. D., Alfarra, M. R., Zhang, Q., et al. (2007). Chemical and Microphysical Characterization of Ambient Aerosols with the Aerodyne Aerosol Mass Spectrometer. *Mass Spectrom. Rev.*, 26:185–222.
- Choel, M., Deboudt, K., Flament, P., Aimoz, L., and Meriaux, X. (2007). Single-Particle Analysis of Atmospheric Aerosols at Cape Gris-Nez, English Channel: Influence of Steel Works on Iron Apportionment. *Atmos. Environ.*, 41:2820–2830.
- Choi, S. D., Baek, S. Y., and Chang, Y. S. (2007). Influence of a Large Steel Complex on the Spatial Distribution of Volatile Polycyclic Aromatic Hydrocarbons (PAHs) Determined by Passive Air Sampling Using Membrane-Enclosed Copolymer (MECOP). *Atmos. Environ.*, 41:6255–6264.
- Dall'Osto, M., Booth, M. J., Smith, W., Fisher, R., and Harrison, R. M. (2008). A Study of the Size Distributions and the Chemical Characterization of Airborne Particles in the Vicinity of a Large Integrated Steelworks. *Aerosol Sci. Technol.*, 42:981–991.
- Dall'Osto, M., and Harrison, R. M. (2006). Chemical Characterisation of Single Airborne Particles in Athens (Greece) by ATOFMS. *Atmos. Environ.*, 40:7614–7631.
- DeCarlo, P. F., Kimmel, J. R., Trimborn, A., Northway, M. J., Jayne, J. T., Aiken, A. C., et al. (2006). Field-Deployable, High-Resolution, Time-of-Flight Aerosol Mass Spectrometer. *Anal. Chem.*, 78:8281–8289.
- Denkenberger, K. A., Moffet, R. C., Holecek, J. C., Rebotier, T. P., and Prather, K. A. (2007). Real-Time, Single-Particle Measurements of Oligomers in Aged Ambient Aerosol Particles. *Environ. Sci. Technol.*, 41:5439–5446.
- Dockery, D. W., Pope, C. A., Xu, X. P., Spengler, J. D., Ware, J. H., et al. (1993). An Association between Air-Pollution and Mortality in 6 United States Cities. *N. Engl. J. Med.*, 329:1753–1759.
- Drewnick, F., Hings, S. S., DeCarlo, P., Jayne, J. T., Gonin, M., Fuhrer, K., et al. (2005). A new Time-of-Flight Aerosol Mass Spectrometer (TOF-AMS) - Instrument Description and First Field Deployment. *Aerosol Sci. Technol.*, 39:637–658.
- Dzepina, K., Arey, J., Marr, L. C., Worsnop, D. R., Salcedo, D., Zhang, Q., et al. (2007). Detection of Particle-Phase Polycyclic Aromatic Hydrocarbons in Mexico City Using an Aerosol Mass Spectrometer. *Int. J. Mass Spectrom.*, 263:152–170.

- Gard, E., Mayer, J. E., Morrical, B. D., Dienes, T., Fergenson, D. P., and Prather, K. A. (1997). Real-Time Analysis of Individual Atmospheric Aerosol Particles: Design and Performance of a Portable ATOFMS. *Anal. Chem.*, 69(20), 4083–4091.
- Gross, D. S., Galli, M. E., Silva, P. J., and Prather, K. A. (2000). Relative Sensitivity Factors for Alkali Metal and Ammonium Cations in Single Particle Aerosol Time-of-Flight Mass Spectra. *Anal. Chem.*, 72, 416–422.
- Gross, D. S., Galli, M. E., Silva, P. J., Wood, S. H., Liu, D. Y., and Prather, K. A. (2000). Single Particle Characterization of Automobile and Diesel Truck Emissions in the Caldecott Tunnel. *Aerosol Sci. Technol.*, 32:152–163.
- Guazzotti, S. A., Coffee, K. R. and Prather, K. A. (2001). Continuous Measurements of Size-Resolved Particle Chemistry during INDOEX Intensive Field Phase 99. *J. Geophys. Res.*, 106(D22):28607–28627.
- Harrison, R. M., and Jones, A. M. (2005). Multisite Study of Particle Number Concentrations in Urban Air. *Environ. Sci. Technol.*, 39:6063–6070.
- Harrison, R. M., Laxen, D., Moorcroft, S., and Laxen, K. (forthcoming). Processes Affecting Concentrations of Fine Particulate Matter (PM_{2.5}) in the UK Atmosphere. *Atmos. Environ.*
- Harrison, R. M., and Yin, J. (2000). Particulate Matter in the Atmosphere: Which Particle Properties Are Important for Its Effects on Health? *Sci. Tot. Environ.*, 249:85–101.
- Hutchison, G., Brown, D. M., Hibbs, L. R., Heal, M. R., Donaldson, K., Maynard, R. L., et al. (2005). The Effect of Refurbishing a UK Steel Plant on PM10 Metal Composition and Ability to Induce Inflammation. *Resp. Res.*, 6:43.
- Jayne, J. T., Leard, D. C., Zhang, X. F., Davidovits, P., Smith, K. A., Kolb, C. E., and Worsnop, D. R. (2000). Development of an Aerosol Mass Spectrometer for Size and Composition Analysis of Submicron Particles. *Aerosol Sci. Tech.*, 33: 49–70.
- Jiun-Hong, T., Kuo-Hsiung, L., Chihyu, C., Jian-Yuan, D., Ching-Guan, C., and Hung-Lung, C. (2007). Chemical Constituents in Particulate Emissions from an Integrated Iron and Steel Facility. *J. Hazard. Mater.*, 147:111–119.
- Khalili, N. R., Scheff, P. A., and Holsen, T. M. (1995). PAH Source Fingerprints for Coke Ovens, Diesel and Gasoline Engines, Highway Tunnels, and Wood Combustion Emissions. *Atmos. Environ.*, 29(4):533–542.
- Kim, Y., and Worrell, E. (2002). International Comparison of CO₂ Emission Trends in the Iron and Steel Industry. *Energy Policy*, 30:827–838.
- Ledoux, F., Laversin, H., Courcot, D., Courcot, L., Zhilinskaya, E. A., Puskaric, E., et al. (2006). Characterization of Iron and Manganese Species in Atmospheric Aerosols from Anthropogenic Sources. *Atmos. Res.*, 82:622–632.
- Liu, D.-Y., Wenzel, R. J., and Prather, K. A. (2003). Aerosol Time-of-Flight Mass Spectrometry during the Atlanta Supersite Experiment: 1. Measurements. *J. Geophys. Res.*, 108(D7):8426.
- Mazzei, F., D'Alessandro, A., Lucarelli, F., Marenco, F., Nava, S., Prati, P., et al. (2006). Elemental Composition and Source Apportionment of Particulate Matter Near a Steel Plant in Genoa (Italy). *Nucl. Instrum. Methods Phys. Res. B - Beam Interact. Mater. Atmos.*, 249:548–551.
- Moffet, R., Shields, L., Bernsten, J., Devlin, R., and Prather, K. (2004). Characterization of an Ambient Coarse Particle Concentrator Used for Human Exposure Studies: Aerosol Size Distributions, Chemical Composition, and Concentration Enrichment. *Aerosol Sci. Technol.*, 38(11):1123–1137.
- Moreno, T., Merolla, L., Gibbons, W., Greenwell, L., Jones, T., and Richards, R. (2004). Variations in the Source, Metal Content and Bioreactivity of Technogenic Aerosols: A Case Study from Port Talbot, Wales, UK. *Sci. Total Environ.*, 333:59–73.
- Murphy, D. M. (2007). The Design of Single Particle Laser Mass Spectrometers. *Mass Spectrom. Rev.*, 26:150–165.
- Noble, C. A., and Prather, K. A. (1996). Real-Time Measurement of Correlated Size and Composition Profiles of Individual Atmospheric Aerosol Particles. *Environ. Sci. Technol.*, 30(9), 2667–2680.
- Ogulei, D., Hopke, P. K., Zhou, L. M., Paatero, P., Park, S. S., and Ondov, J. (2005). Receptor Modeling for Multiple Time Resolved Species: The Baltimore Supersite. *Atmos. Environ.*, 39:3751–3762.
- Oravisarjari, K., Timonen, K. L., Wiikinkoski, T., Ruuskanen, A. R., Heinanen, K., and Ruuskanen, J. (2003). Source Contributions to PM_{2.5} Particles in the Urban Air of a Town Situated Close to a Steel Works. *Atmos. Environ.*, 37:1013–1022.
- Pastor, S. H., Allen, J. O., Hughes, L. S., Bhawe, P., Cass, G. R., and Prather, K. A. (2003). Ambient Single Particle Analysis in Riverside, California by Aerosol Time-of-Flight Mass Spectrometry during the SCOS97-NARSTO. *Atmos. Environ.*, 37:239–258.
- Pope, C. A. (1996). Particulate Pollution and Health: A Review of the Utah Valley Experience. *J. Exp. Anal. Environ. Epidemiol.*, 6:23–34.
- Pope, C. A., Burnett, R. T., Thun, M. J., Calle, E. E., Krewski, D., Ito, K., et al. (2002). Lung cancer, cardiopulmonary mortality, and long-term exposure to fine particulate air pollution. *JAMA*, 287:1132–1141.
- Pope, C. A., Thun, M. J., Namboodiri, M. M., Dockery, D. W., Evans, J. S., Speizer, F. E., et al. (1995). Particulate Air Pollution as a Predictor of Mortality in a Prospective Study of US Adults. *Am. J. Respir. Crit. Care Med.*, 151(3):669–674.
- Qin, X. Y., Bnave, P. V., and Prather, K. A. (2006). Comparison of Two Methods for Obtaining Quantitative Mass Concentrations from Aerosol Time-of-Flight Mass Spectrometry Measurements. *Anal. Chem.*, 78:6169–6178.
- Qin, X. Y., and Prather, K. A. (2006). Impact of Biomass Emissions on Particle Chemistry during the California Regional Particulate Air Quality Study. *Int. J. Mass Spectrom.*, 258:142–150.
- Rebotier, T. P., and Prather, K. A. (2007). Aerosol Time-of-Flight Mass Spectrometry Data Analysis: A Benchmark of Clustering Algorithms. *Analytica Chimica Acta.*, 585:38–54.
- Silva, P. J., and Prather, K. A. (2000). Interpretation of Mass Spectra from Organic Compounds in Aerosol Time-of-Flight Mass Spectrometry. *Anal. Chem.*, 72:3553–3562.
- Song, X. H., Hopke, P. K., Fergenson, D. P., and Prather, K. A. (1999). Classification of Single Particles Analyzed by ATOFMS Using an Artificial Neural Network, ART-2A. *Anal. Chem.*, 71:860–865.
- Su, Y. X., Sipin, M. F., Furutani, H., and Prather, K. A. (2004). Development and Characterization of an Aerosol Time-of-Flight Mass Spectrometer with Increased Detection Efficiency. *Anal. Chem.*, 76(3):712–719.
- Thompson, P., Anderson, D. R., Fisher, R., Thompson, D., and Sharp, J. H. (2003). Process-Related Patterns in Dioxin Emissions: A Simplified Assessment Procedure Applied to Coke Combustion in Sinter Plant. *Fuel*, 82:2125–2137.
- Wang, L. C., Lee, W. J., Tsai, P. J., Lee, W. S., and Chang-Chien, G. P. (2003). Emissions of Polychlorinated Dibenzo-p-Dioxins and Dibenzofurans from Stack Flue Gases of Sinter Plants. *Chemosphere*, 50:1123–1129.
- Wang, T. S., Anderson, D. R., Thompson, D., Clench, M., and Fisher, R. (2003). Studies into the Formation of Dioxins in the Sintering Process Used in the Iron and Steel Industry. 1. Characterisation of Isomer Profiles in Particulate and Gaseous Emissions. *Chemosphere*, 51:585–594
- Weitkamp, E. A., Lipsky, E. M., Pancras, P. J., Ondov, J. M., Polidori, A., Turpin, B. J., et al. (2005). Fine Particle Emission Profile for a Large Coke Production Facility Based on Highly Time-Resolved Fence Line Measurements. *Atmos. Environ.*, 39:6719–6733.
- Yang, H. H., Lai, S. O., Hsieh, L. T., Hsueh, H. J., and Chi, T. W. (2002). Profiles of PAH Emission from Steel and Iron Industries. *Chemosphere*, 48:1061–1074.
- Yang, H. H., Lee, W. J., Chena, S. J., and Lai, S. O. (1998). PAH Emission from Various Industrial Stacks. *J. Hazard. Mater.*, 60:159–174.